

Supporting Information

Photophysical Reappraisal of Additives for Photovoltaic Systems: A Case Study on Three Hole Transporting Materials and Two Dopants

Sergio Ramírez-Barroso,^a Jorge Marco-Guimbao,^a David García-Fresnadillo,^{*b} Nazario Martín,^{b,c} and Juan Luis Delgado^{*a}

^a*POLYMAT, University of the Basque Country UPV/EHU, 72, Avenida de Tolosa, Donostia-San Sebastian, 20018, Spain.* ^b*Department of Organic Chemistry, Faculty of Chemical Sciences, Complutense University of Madrid, Avenida Complutense s/n, Madrid, 28040, Spain.* ^c*IMDEA Nanoscience Institute, C/ Faraday, 9, Campus de Cantoblanco, Madrid, 28049, Spain.*

Table of Contents

1. UV-Vis absorption spectra	1
2. Excitation and emission spectra.....	4
3. Fluorescence decays	7
4. Fluorescence anisotropy	11
5. Singlet oxygen production	11

1. UV-Vis absorption spectra

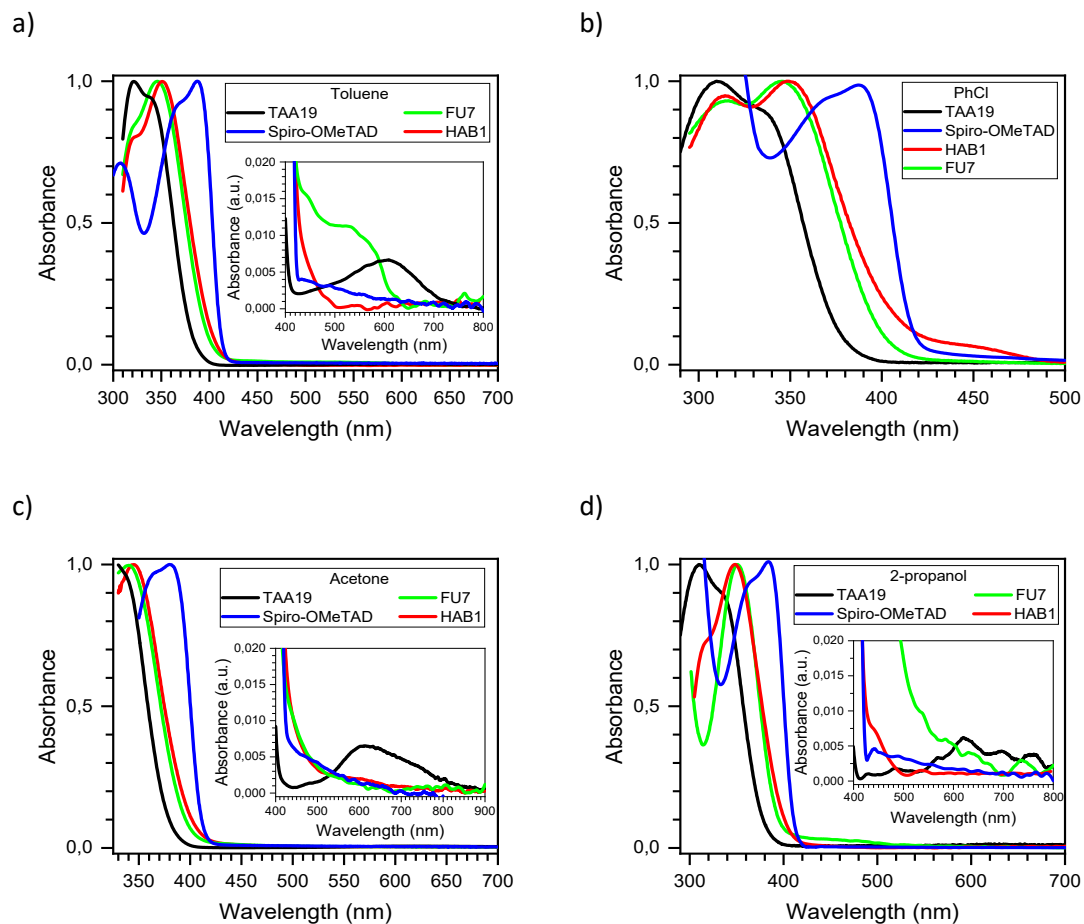


Figure S1. Comparison of the normalised UV-Vis absorption spectra of **TAA19**, **HAB1**, **FU7** and **Spiro-OMeTAD** solutions (2x10⁻⁶ M) at room temperature (25±2 °C) in air-equilibrated solvents: a) toluene, b) chlorobenzene, c) acetone and d) 2-propanol.

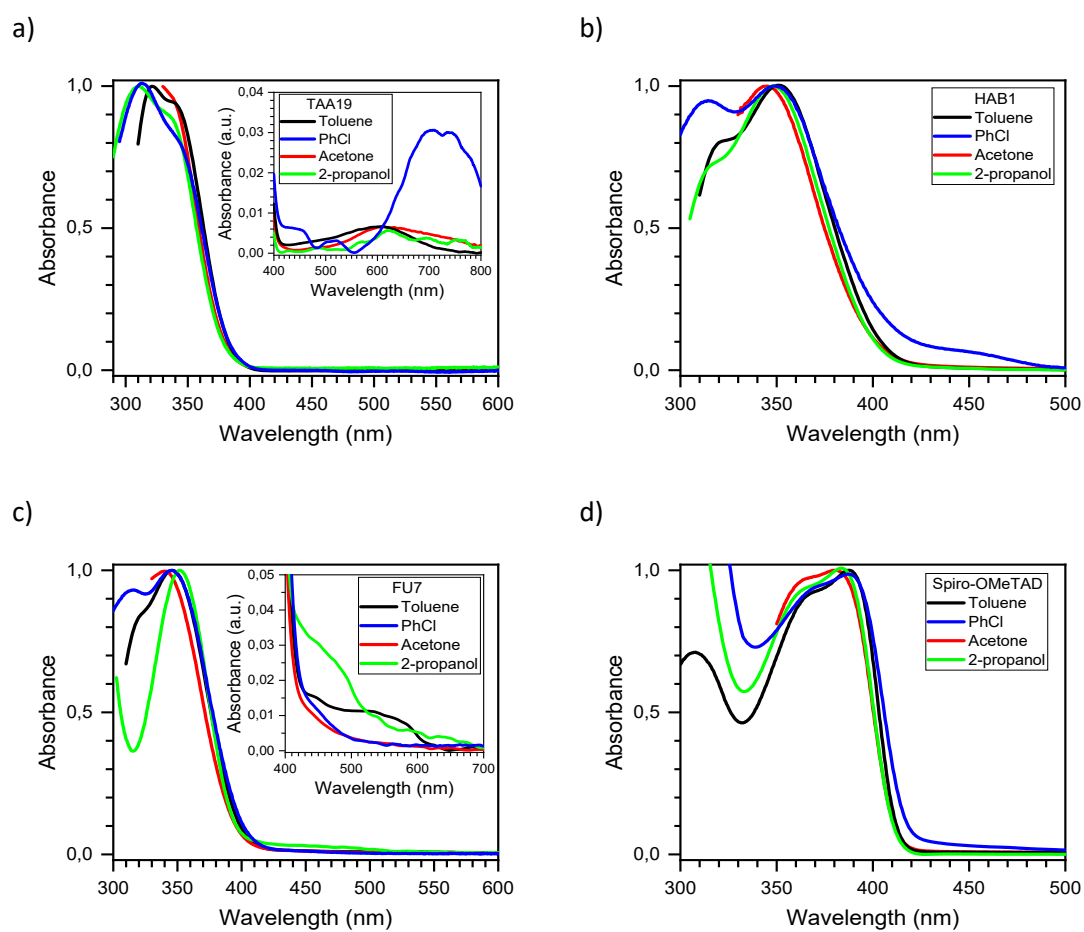


Figure S2. Comparison of the normalised UV-Vis absorption spectra of **TAA19** (a), **HAB1** (b), **FU7** (c) and **Spiro-OMeTAD** (d) solutions (2×10^{-6} M), at room temperature (25 ± 2 °C), in the air-equilibrated solvents assayed: toluene, chlorobenzene, acetone and 2-propanol.

Table S1. Wavelength of the absorption peaks and shoulders (sh) and molar absorption coefficients of **TAA19**, **HAB1**, **FU7** and **Spiro-OMeTAD** (2×10^{-6} M) at room temperature (25 ± 2 °C) in toluene, acetone, 2-propanol, and chlorobenzene either with or without **FK209** (6×10^{-8} M) or **Li-TFSI** (1×10^{-6} M) + **TBP** (6×10^{-6} M).

Sample	Solvent	$\lambda_{\text{abs}} / \text{nm} (\epsilon / \text{M}^{-1}\text{cm}^{-1})^a$
TAA19	Toluene	321 (51300), 337sh (48400), 608 (342)
	Acetone	<330 nm, ^b 612 (285)
	2-Propanol	310 (48600), 336sh (43400), 621 (300)
	PhCl	313 (56500), 341 (46300), 705 (1730)
HAB1	Toluene	323sh (48500), 351 (60300)
	Acetone	345 (52400)
	2-Propanol	315sh (33900), 348 (47350)
	PhCl	315 (61400), 349 (64650), 443sh (4550)
	PhCl with FK209	348 (24600), 517 (1400), 590sh (680)
	PhCl with LiTFSI+TBP	347 (50430), 517 (1550),
FU7	Toluene	323sh (38000), 346 (44700), 440 (698), 522 (504)
	Acetone	340 (38500)
	2-Propanol	351 (32200), 466sh (870)
	PhCl	316 (45900), 345 (49300),
	PhCl with FK209	346 (31500)
	PhCl with LiTFSI+TBP	343sh (7300)
Spiro-OMeTAD	Toluene	308 (47000), 371sh (61900), 388 (66700)
	Acetone	370sh (67000), 380 (68500)
	2-Propanol	362sh (55300), 385 (62000)
	PhCl	375sh (64100), 388 (67600)
	PhCl with FK209	369 (25300), 499sh (14700), 525 (16600)
	PhCl with LiTFSI+TBP	370sh (42200), 387 (41800)

^a Experimental uncertainty: ± 3 nm ($\pm 15\%$). ^b Solvent cutoff wavelength for acetone is 330 nm (wavelength at which the solvent absorbance in a 1 cm path length cell is equal to 1 absorbance unit).

2. Excitation and emission spectra

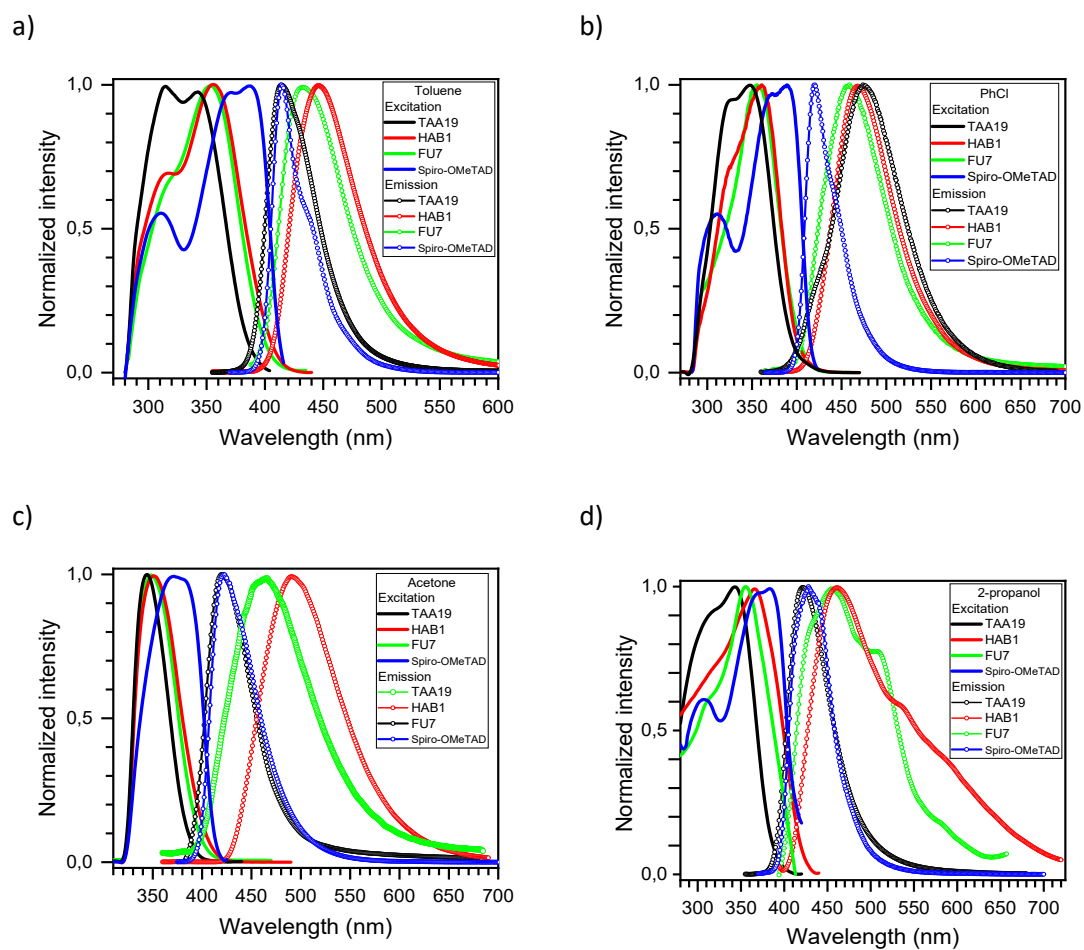


Figure S3. Comparison of the normalised UV-Vis excitation and fluorescence spectra of **TAA19**, **HAB1**, **FU7** and **Spiro-OMeTAD** solutions (2×10^{-6} M) at room temperature (25 ± 0.2 °C) in air-equilibrated solvents: a) toluene, b) chlorobenzene, c) acetone and d) 2-propanol. Emission spectra were acquired with $\lambda_{\text{exc}}^{\text{max}}$, while the excitation spectra were recorded at $\lambda_{\text{em}}^{\text{max}}$.

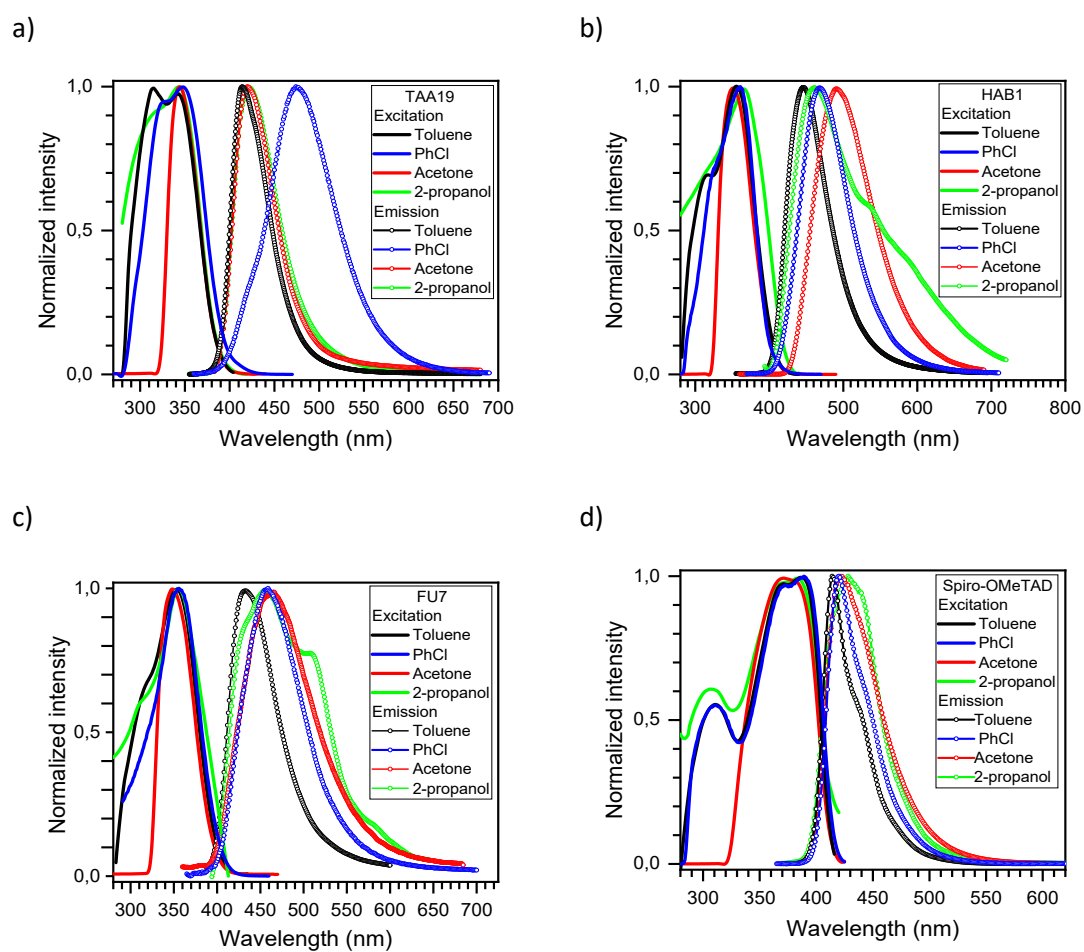


Figure S4. Comparison of the normalised UV-Vis excitation and emission spectra of **TAA19** (a), **HAB1** (b), **FU7** (c) and **Spiro-OMeTAD** (d) solutions (2×10^{-6} M), at room temperature (25 ± 0.2 °C) in the air-equilibrated solvents assayed: toluene, chlorobenzene, acetone and 2-propanol. Emission spectra were acquired with λ_{exc}^{max} , while the excitation spectra were recorded at λ_{em}^{max} . The excitation spectra in acetone are affected by the cut-off wavelength of the solvent (330 nm) on its left-hand side.

Table S2. Excitation ($\lambda_{\text{exc}}^{\text{max}}$) and emission ($\lambda_{\text{em}}^{\text{max}}$) peaks and shoulders (sh), full width at half maximum (FWHM), Stokes shifts, optical energy gap and fluorescence quantum yields of **TAA19**, **HAB1**, **FU7** and **Spiro-OMeTAD** (2×10^{-6} M) at room temperature (25 ± 0.2 °C) in air-equilibrated toluene, acetone, 2-propanol, and chlorobenzene either with or without **FK209** (6×10^{-8} M) or **Li-TFSI** (1×10^{-6} M) + **TBP** (6×10^{-6} M).

Sample	Solvent	$\lambda_{\text{exc}}^{\text{max}}$ nm ^a	$\lambda_{\text{em}}^{\text{max}}$ nm ^a	FWHM cm ⁻¹ (eV)	Stokes shift cm ⁻¹ (eV)	E_{0-0} ^b eV	Φ_{em} ^c
TAA19	Toluene	315, 342	414	2682 (0.33)	5085 (0.63)	3.20	0.055
	Acetone	344	420	2891 (0.36)	5260 (0.65)	3.19	0.016
	2-Propanol	312sh, 343	420	3066 (0.38)	5345 (0.66)	3.19	0.012
	PhCl	326sh, 348	425sh, 474	3739 (0.46)	7639 (0.95)	3.10	0.19
HAB1	Toluene	318sh, 355	446	3205 (0.40)	5772 (0.72)	3.05	0.15
	Acetone	350	491	3672 (0.46)	8205 (1.02)	2.93	0.23
	2-Propanol	366	461, 535sh, 577sh	5352 (0.66)	5631 (0.70)	2.99	0.12
	PhCl	323sh, 361	467	3420 (0.42)	6288 (0.78)	3.02	0.19
	PhCl / FK209	325, 370sh, 397	467sh, 474, 511sh, 573sh	5093 (1.07)	4092 (0.51)	2.98	0.002
	PhCl / LiTFSI+TBP	321sh, 364	467, 474sh	3496 (0.43)	6151 (0.76)	2.98	0.022
FU7	Toluene	317sh, 353	433	3249 (0.40)	5234 (0.65)	3.11	0.022
	Acetone	348	465	4387 (0.54)	7230 (0.90)	3.11	0.009
	2-Propanol	312sh, 356	455, 504sh, 579sh	5320 (0.66)	6112 (0.76)	3.07	0.007
	PhCl	356	459	3822 (0.47)	6303 (0.78)	3.06	0.040
	PhCl / FK209	327sh, 357	450	3788 (0.47)	5789 (0.72)	3.06	0.004
	PhCl / LiTFSI+TBP	329sh, 356	451	4213 (0.52)	5838 (0.72)	3.08	0.002
Spiro-OMeTAD	Toluene	311, 371, 387	414, 435sh	2016 (0.25)	1685 (0.21)	3.06	0.26
	Acetone	371, 383sh	422, 434sh	2792 (0.35)	2413 (0.30)	3.06	0.45
	2-Propanol	307, 371sh, 383	429, 439sh	2842 (0.35)	2800 (0.35)	3.06	0.42
	PhCl	311, 372, 389	420, 439sh	2233 (0.28)	1897 (0.24)	3.04	0.35
	PhCl / FK209	310, 362, 408	399sh, 435, 450sh, 536sh, 592sh, 622sh	7956 (0.99)	1521 (0.19)	2.92	0.02
	PhCl / LiTFSI+TBP	317, 372, 390	419, 439sh	2258 (0.28)	1774 (0.22)	3.04	0.30

^a Experimental uncertainty: ± 1 nm. ^b Experimental uncertainty: ± 0.01 eV. ^c Argon-purged solution. Experimental uncertainty: $\pm 10\%$.

3. Fluorescence decays

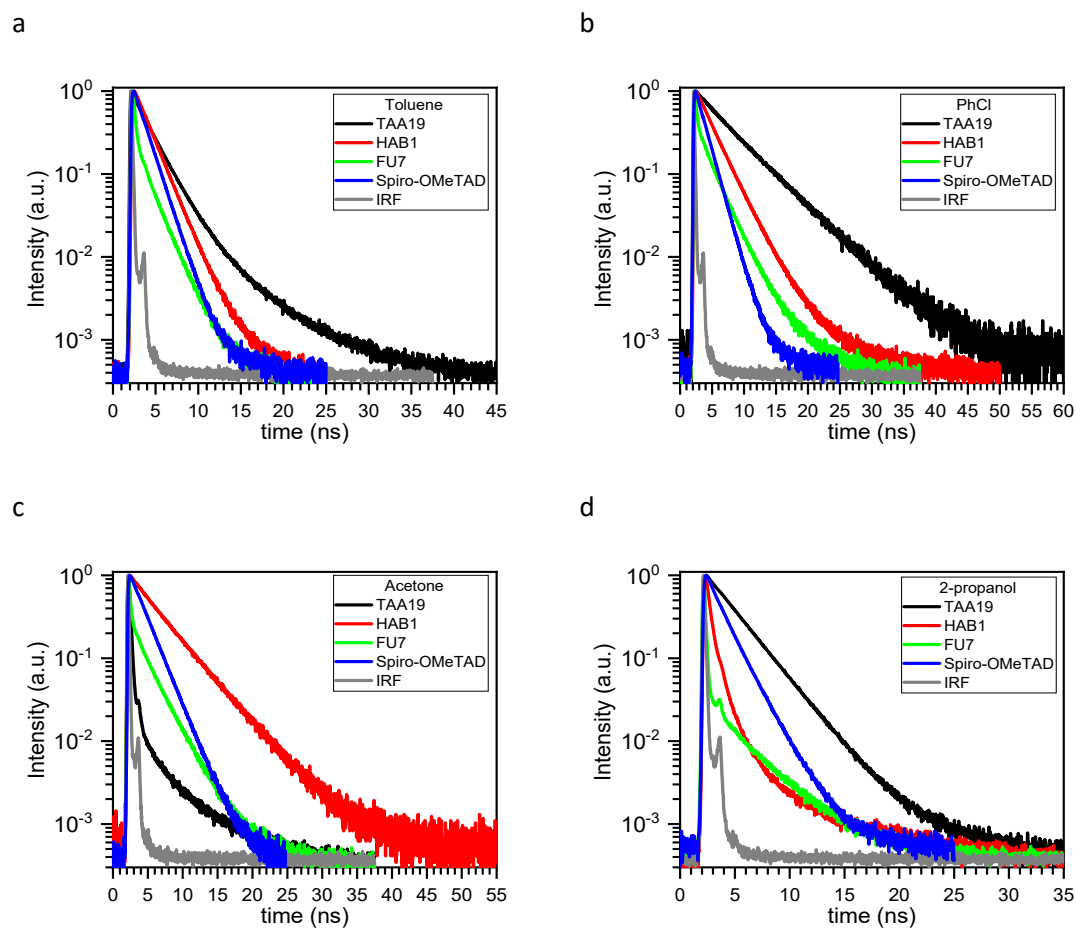


Figure S5. Fluorescence decays recorded at the position of the emission maximum of **TAA19**, **HAB1**, **FU7** and **Spiro-OMeTAD** (2×10^{-6} M) at room temperature (25 ± 0.2 °C) in air-equilibrated toluene (a), chlorobenzene (b), acetone (c) and 2-propanol (d). $\lambda_{\text{exc}} = 373$ nm. IRF stands for instrument response function.

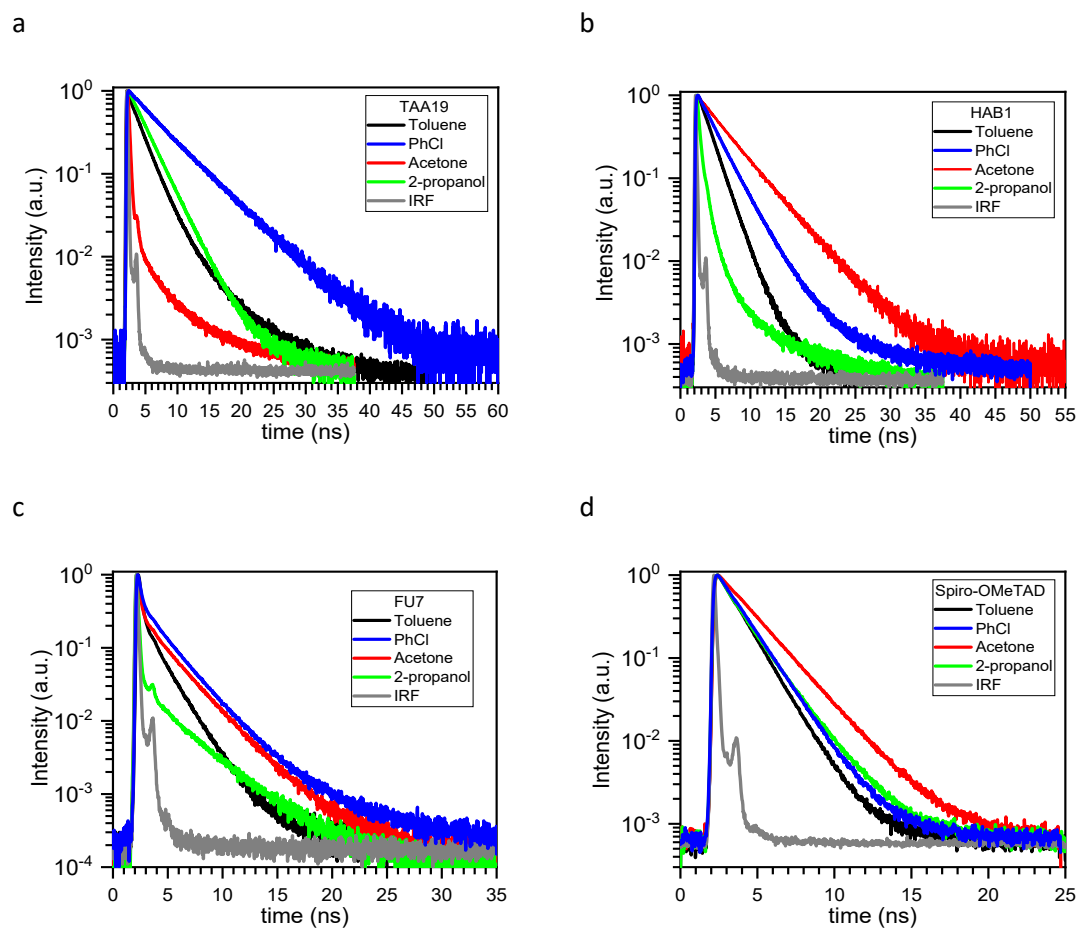


Figure S6. Fluorescence decays recorded at the position of the emission maximum of **TAA19**, **HAB1**, **FU7** and **Spiro-OMeTAD** (2×10^{-6} M) at room temperature (25 ± 0.2 °C) in air-equilibrated toluene (a), chlorobenzene (b), acetone (c) and 2-propanol (d). $\lambda_{\text{exc}} = 373$ nm. IRF stands for instrument response function.

Table S3. Data from the fitting to multiexponential functions of the photoluminescence decays of **TAA19**, **HAB1**, **FU7** and **Spiro-OMeTAD** (2×10^{-6} M) in toluene, acetone, 2-propanol, and chlorobenzene either with or without **FK209** (6×10^{-8} M) or **Li-TFSI** (1×10^{-6} M) + **TBP** (6×10^{-6} M) at room temperature (25 ± 0.2 °C) in air-equilibrated conditions, with excitation at 373 nm and detection at the corresponding emission maximum.

Sample	Solvent	A_1^a %	I_1^b %	τ_1^c ns	A_2^a %	I_2^b %	τ_2^c ns	A_3^a %	I_3^b %	τ_3^c ns	τ_{INT}^d ns	τ_{AMP}^e ns	X^2
TAA19	Toluene	0.05	0.12	5.70	0.95	0.88	2.03				2.46	2.19	1.085
	Acetone	0.01	0.07	6.48	0.01	0.06	1.74	0.98	0.87	0.20	0.74	0.23	1.125
	2-propanol	0.01	0.02	7.50	0.84	0.97	2.56	0.15	0.02	0.24	2.61	2.24	1.153
	PhCl	0.80	0.91	5.81	0.20	0.09	2.27				5.50	5.10	1.095
HAB1	Toluene	0.01	0.02	4.82	0.99	0.98	1.66				1.72	1.68	1.131
	Acetone	0.81	0.91	4.54	0.19	0.08	1.84				4.22	3.96	1.147
	2-propanol	0.01	0.06	5.15	0.14	0.32	0.93	0.85	0.62	0.29	0.77	0.40	1.078
	PhCl ^f	0.02	0.04	5.92	0.98	0.96	2.87				2.99	2.93	1.179
	PhCl	0.06	0.10	4.94	0.94	0.90	2.41				2.61	2.53	1.253
	PhCl with FK209	0.07	0.12	4.24	0.93	0.88	2.37				2.59	2.50	1.113
	PhCl with LiTFSI+TBP	0.04	0.07	4.90	0.96	0.93	2.37				2.56	2.47	1.092
FU7	Toluene	0.08	0.42	1.88	0.08	0.18	0.87	0.84	0.40	0.17	1.01	0.36	1.119
	Acetone	0.10	0.58	2.76	0.07	0.14	0.95	0.83	0.28	0.15	1.79	0.46	1.139
	2-propanol	0.01	0.13	3.75	0.01	0.03	1.13	0.98	0.84	0.06	0.57	0.07	1.164
	PhCl ^f	0.02	0.10	5.39	0.08	0.42	1.94	0.90	0.48	0.20	1.45	0.44	1.136
	PhCl	0.02	0.16	3.81	0.09	0.39	1.65	0.89	0.44	0.19	1.36	0.38	1.111
	PhCl with FK209	0.02	0.18	4.09	0.10	0.45	1.65	0.88	0.37	0.15	1.52	0.36	1.166
	PhCl with LiTFSI+TBP	0.04	0.25	2.51	0.09	0.32	1.42	0.87	0.43	0.19	1.17	0.39	1.185
Spiro-OMeTAD	Toluene	0.75	0.82	1.42	0.25	0.18	0.97	-	-	-	1.34	1.31	1.087
	Acetone	0.94	0.98	2.07	0.06	0.02	0.65	-	-	-	2.04	1.97	1.071
	2-propanol	0.56	0.73	1.78	0.44	0.27	0.86	-	-	-	1.53	1.37	1.086
	PhCl ^f	1.00	1.00	1.78							1.78 ^g	1.78 ^g	1.093
	PhCl	1.00	1.00	1.62							1.62 ^g	1.62 ^g	1.239
	PhCl with FK209	0.84	0.91	1.61	0.15	0.08	0.76	0.01	0.01	7.93	1.58	1.53	1.083
	PhCl with LiTFSI+TBP	0.61	0.68	1.66	0.39	0.32	1.21	-	-	-	1.52	1.48	1.123

^a Relative amplitude-based preexponential factor. ^b Relative intensity-based preexponential factor. ^c Discrete lifetime component. ^d Intensity-weighted average emission lifetime. Experimental uncertainty: ± 10 –20%. ^e Amplitude-weighted average emission lifetime. Experimental uncertainty: ± 10 –20%. ^f Ar-purged sample. ^g A single exponential function was sufficient for accurate fit of the fluorescence decay.

Table S4. Intensity-weighted average fluorescence lifetimes, dynamic bimolecular deactivation rate constants for fluorescence quenching by **FK209** or **Li-TFSI + TBP** of **HAB1**, **FU7** and **Spiro-OMeTAD**, and association constants of **FK209** to **HAB1**, **FU7** and **Spiro-OMeTAD** in Ar-purged chlorobenzene (HTMs concentration 2×10^{-6} M), determined at 373 nm excitation wavelength.

Sample	$\tau_{0_{INT}}$ [ns]	$k_q^S \tau_{0_{INT}} [M^{-1}s^{-1}]^a$	$k_q^S \omega_{em} [M^{-1}s^{-1}]^a$	$K_a [M^{-1}]^b$
HAB1 with FK209	2.99 ± 0.32	$2.8 \cdot 10^{10} (\pm 3\%)$	-	$6.1 \cdot 10^2 (\pm 20\%)$
HAB1 with Li-TFSI+TBP		$4.3 \cdot 10^9 (\pm 6\%)$	$4.8 \cdot 10^9 (\pm 6\%)$	-
FU7 with FK209	1.45 ± 0.16	$2.1 \cdot 10^9 (\pm 3\%)$	-	$8.2 \cdot 10^2 (\pm 32\%)$
FU7 with Li-TFSI+TBP		$3.1 \cdot 10^9 (\pm 2\%)$	$3.7 \cdot 10^9 (\pm 2\%)$	-
Spiro-OMeTAD with FK209	1.78 ± 0.21	$4.1 \cdot 10^{10} (\pm 2\%)$	-	$9.6 \cdot 10^2 (\pm 29\%)$
Spiro-OMeTAD with Li-TFSI+TBP		$4.5 \cdot 10^9 (\pm 2\%)$	$5.3 \cdot 10^9 (\pm 2\%)$	-

^a Relative error of the slopes obtained by linear regression in parentheses. ^b K_a values obtained by fitting the experimental data points of the corresponding Stern-Volmer plots to the equation below, that is the most general approach to static quenching upon adduct formation resulting in an intensity change caused by association (see reference 103 of the manuscript):

$$\frac{I_0 - [F]_t}{I} = \frac{[F]_t}{\left\{ [F]_t + \left(\frac{\varphi_A - \varphi_F}{\varphi_F} \right) \left([F]_t + [Q]_t + \frac{1}{K_a} - \sqrt{\left([F]_t + [Q]_t + \frac{1}{K_a} \right)^2 - 4[F]_t \times [Q]_t} \right) \right\}}$$

where I_0 and I are the fluorescence intensities in the presence and absence of the quencher, respectively, $[F]$ is the total concentration of the fluorophore (bound plus unbound), φ_A and φ_F are values proportional to the fluorescence intensity or quantum yield at the observed emission wavelength of the associated complex (A), and the fluorophore (F), respectively, under the same experimental conditions; and $[Q]$ is the total concentration of the quencher.

4. Fluorescence anisotropy

Table S5. Data from the time-resolved fluorescence anisotropy experiments. Fluorophore rotational lifetime (τ_{rot}), hydrodynamic volume and hydrodynamic diameter of **HAB1**, **FU7** and **Spiro-OMeTAD** (2×10^{-6} M) in chlorobenzene either with or without **FK209** (6×10^{-8} M) or **Li-TFSI** (1×10^{-6} M) + **TBP** (6×10^{-6} M) at room temperature (25 ± 0.2 °C) in air-equilibrated conditions, with excitation at 373 nm and detection at the corresponding emission maximum.

Sample	τ_{rot}^a ns	Hydrodynamic Volume ^b nm ³	Hydrodynamic Diameter ^c nm
HAB1	0.297	1.62	1.46
HAB1 with FK209	1.71	9.34	2.61
HAB1 with LiTFSI+TBP	0.276	1.51	1.42
FU7	0.786	4.29	2.02
FU7 with FK209	3.009	16.43	3.15
FU7 with LiTFSI+TBP	0.643	3.51	1.89
Spiro-OMeTAD	0.458	2.50	1.68
Spiro-OMeTAD with FK209	2.180	11.91	2.83
Spiro-OMeTAD with LiTFSI+TBP	0.482	2.63	1.71

^a Experimental uncertainty: $\pm 15\%$. ^b Experimental uncertainty: ± 0.50 nm³. ^c Experimental uncertainty: ± 0.15 nm.

5. Singlet oxygen production

Table S6. Absorbance at the excitation wavelength of the HTMs solutions used in the singlet oxygen quantification experiments, singlet oxygen phosphorescence lifetimes (τ_{Δ}), phosphorescence signal at zero time (S_0) and quantum yields and of singlet oxygen production (Φ_{Δ}) by **HAB1**, **FU7**, **Spiro-OMeTAD** (2×10^{-6} M) and phenalen-1-one in air-equilibrated chlorobenzene either with or without **FK209** (6×10^{-8} M) or **Li-TFSI** (1×10^{-6} M) + **TBP** (6×10^{-6} M) at room temperature (25 ± 0.2 °C), with excitation at 373 nm and detection at 1270 nm.

Sample	Absorbance at 373 nm	τ_{Δ} ¹ O ₂ μs	S_0	Φ_{Δ}
HAB1	0.1271	42.60	105476	0.057
HAB1 with FK209	0.0983	41.85	62894	0.032
HAB1 with LiTFSI+TBP	0.1035	42.13	87531	0.045
FU7	0.1050	42.48	36898	0.019
FU7 with FK209	0.1195	42.06	42562	0.022
FU7 with LiTFSI+TBP	0.0986	41.99	34849	0.017
Spiro-OMeTAD	0.1931	42.11	1126336	0.347
Spiro-OMeTAD with FK209	0.1853	41.91	657304	0.211
Spiro-OMeTAD with LiTFSI+TBP	0.1892	42.02	1008220	0.317
Phenalen-1-one	0.1118	42.63	1879391	1.00